Strengthening the Bridge Between Chiral Lagrangians and QCD Sum-Rules

Jason Ho

Dordt University

QCD2025
Montpellier, France

Outline

The Scalar Mesons

- Understanding the light scalar sector of QCD has long been a challenging problem
  - *e.g.*, mixing of quark and glue components, other complex nonperturbative dynamics
- The experimental data in this low-energy region has also proved challenging
  - *e.g.*, wide, overlapping resonances, low resolution
- Chiral Lagrangian models (LSM, NLSM) have been valuable tools for understanding this sector.

Bridging Chiral Lagrangians and QCD Sum-Rules

- **Chiral Lagrangians** consider effective hadronic fields
  - Chiral Lagrangians have model parameters fixed by low-energy experimental data.
  - Generalized linear sigma model (GLSM)
- **QCD Sum-rules** consider hadronic operators built out of constituent quark fields.
  - Quark operators directly probe hadronic substructure.
  - Gaussian sum-rules weigh different energy regimes equally.
- **Can we connect these methodologies to complement one another?**

Amir H. Fariborz, A. Pokraka, T.G. Steele. Mod. Phys. Lett. A31 (2016) 1650023. arXiv:1505.05553

Amir H. Fariborz, **JH**, T.G. Steele. Mod. Phys. Lett. A35 (2020) 2050173. arXiv:1911.04945

Early Methodology

1. Model two-quark ($\bar{q}q$) and four-quark ($\bar{q}q\bar{q}q$) chiral nonets with GLSM
2. Relate physical chiral Lagrangian fields to QCD composite operators via scale factor matrix I and chiral Lagrangian rotation matrix L
3. Impose off-diagonal condition on QCD correlator matrix.
4. Model hadronic side of QCDSR with Breit-Wigner resonance + continuum model with experimental inputs.
5. Solve for scale factors Λ and Λ' and determine energy-dependent behavior.

Early Methodology

Chiral Lagrangian fields describing quark-antiquark scalar nonet M and four-quark nonets M'

$$M = S + i\phi\,,\ M' = S' + i\phi'$$

which have different transformation properties under $U_A(1)$,

$$M \to e^{2i\nu} M, \qquad M' \to e^{-4i\nu} M$$

The scalar nonets $\{S, S'\}$ are given by

$$S = \begin{pmatrix} S_1^1 & a_0^+ & \kappa^+ \\ a_0^- & S_2^2 & \kappa^0 \\ \kappa^- & \bar{\kappa}^0 & S_3^3 \end{pmatrix}\,,\ S' = \begin{pmatrix} {S'}_1^1 & {a'}_0^+ & {\kappa'}^+ \\ {a'}_0^- & {S'}_2^2 & {\kappa'}^0 \\ {\kappa'}^- & \bar{\kappa}'^0 & {S'}_3^3 \end{pmatrix}$$

Early Methodology

We can define these nonets in terms of quark-level operators as well

$$M_{\mathrm{QCD}} = S_{\mathrm{QCD}} + i\phi_{\mathrm{QCD}}\,, \;\; M'_{\mathrm{QCD}} = S'_{\mathrm{QCD}} + i\phi'_{\mathrm{QCD}}$$

where the scalar nonets $\{S_{\mathrm{QCD}}, S'_{\mathrm{QCD}}\}$ are given by composite operators instead,

$$S_{\mathrm{QCD}} = \begin{pmatrix} J_1^{11} & J_1^{a_0^+} & J_1^{\kappa^+} \\ J_1^{a_0^-} & J_1^{22} & J_1^{\kappa^0} \\ J_1^{\kappa^-} & J_1^{\bar{\kappa}^0} & J_1^{33} \end{pmatrix}, \;\; S'_{\mathrm{QCD}} = \begin{pmatrix} J_2^{11} & J_2^{{a'}_0^+} & J_2^{{\kappa'}^+} \\ J_2^{{a'}_0^-} & J_2^{22} & J_2^{{\kappa'}^0} \\ J_2^{{\kappa'}^-} & J_2^{\bar{\kappa}'^0} & J_2^{33} \end{pmatrix}$$

Early Methodology

We relate the physical mesonic states to the chiral Lagrangian operators and the composite quark operators J^{QCD} through a scale factor matrix I and a rotation matrix L

$$\text{Isodoublet}\,(I = 1/2, J = 0): \quad \begin{pmatrix} K_0^*(700) \\ K_0^*(1430) \end{pmatrix} = L_\kappa^{-1} \begin{pmatrix} S_2^3 \\ (S')_2^3 \end{pmatrix} = L_\kappa^{-1} I_\kappa J_\kappa^{\mathrm{QCD}}$$

$$\text{Isotriplet}\,(I = 1, J = 0): \quad \begin{pmatrix} a_0^0(980) \\ a_0^0(1450) \end{pmatrix} = L_a^{-1} \begin{pmatrix} \frac{S_1^1 - S_2^2}{\sqrt{2}} \\ \frac{S'^1_1 - S'^2_2}{\sqrt{2}} \end{pmatrix} = L_a^{-1} I_a J_a^{\mathrm{QCD}}$$

Early Methodology

We relate the physical mesonic states to the chiral Lagrangian operators and the composite quark operators J^{QCD} through a scale factor matrix I and a rotation matrix L

$$L_{\kappa}^{-1} = \begin{pmatrix} \cos\theta_{\kappa} & -\sin\theta_{\kappa} \\ \sin\theta_{\kappa} & \cos\theta_{\kappa} \end{pmatrix}$$

$$L_{a}^{-1} = \begin{pmatrix} \cos\theta_{a} & -\sin\theta_{a} \\ \sin\theta_{a} & \cos\theta_{a} \end{pmatrix} , \quad I_a = I_{\kappa} = \begin{pmatrix} \frac{-m_q}{\Lambda^3} & 0 \\ 0 & \frac{1}{\Lambda'^5} \end{pmatrix}$$

QCDSR Limitations

- For resonances involving complex mixing or involving nonconventional substructure, QCD operators should reflect the mixed content
- Usually the hadronic side of QCDSR is modeled with a resonance + continuum model, typically using a single-narrow resonance (or Breit-Wigner)

For a full multiplet analysis, it will be necessary to account for **wide resonances** and **mixing**.

Revised Methodology

1. Model two-quark ($\bar{q}q$) and four-quark ($\bar{q}q\bar{q}q$) chiral nonets with GLSM
2. Relate physical chiral Lagrangian fields to QCD composite operators via scale factor matrix I_κ and chiral Lagrangian rotation matrix L_κ
3. ~~Impose off-diagonal condition on QCD correlator matrix.~~
4. Model hadronic side of QCDSR with modified BW informed by background-resonance interference approximation.
5. Solve for scale factors Λ and Λ' and determine energy-dependent behavior. Compare predictions for various resonance models.

Amir H. Fariborz, **JH**, T.G. Steele. Phys. Rev. D 111, 094023. arXiv:2501.12601

Background-Resonance Interference Approximation

- Previous work with GLSMs have demonstrated unitarized πK scattering amplitudes can be approximated by a two pole + background model

$$T_0^{1/2}(s) = \frac{\rho(s)}{2}\left[C_\kappa + \sum_{i=1}^{2} \frac{A_{\kappa_i}\left(2m_{\kappa_i}\Gamma_{\kappa_i}\right)}{\rho_{0i}(m_{\kappa_i}^2 - s) - i m_{\kappa_i}\Gamma_{\kappa_i}\rho_{0i}}\right],$$

where $\rho(s) = \frac{q}{8\pi\sqrt{s}} = \frac{\sqrt{[s-(m_\pi+m_K)^2][s-(m_\pi-m_K)^2]}}{16\pi s}$

- The **background-resonance interference approximation** extends this model by including complex fitting coefficients $\{C_\kappa, A_{\kappa_i}\}$

Background-Resonance Interference Approximation

- Additionally, we can modify the fitting model to unitarize each complex-weighted resonance contribution to the amplitude

$$T_0^{1/2}(s) = \frac{\rho(s)}{2}\left[C_\kappa + \sum_{i=1}^{2} \frac{A_{\kappa_i}\left(2m_{\kappa_i}\Gamma_{\kappa_i}\right)}{\rho_{0i}(m_{\kappa_i}^2 - s) - i m_{\kappa_i}\Gamma_{\kappa_i}\rho(s)}\right],$$

  adding an energy-dependent imaginary part.
- Models are fit to πK scattering data[1]

[1] D. Aston, *et al.*, Nucl. Phys. B 296, 493 (1988)

Resonance Modeling: Isodoublets

- Fits to data is good for both models, with similar fitting coefficients.
- $\Delta\delta_0^{1/2}$ is a measure of average relative error of phase shift.

Parameter	Model 1	Model 2
A_{κ_1}	$-0.0560 - i\,0.144$	$-0.0559 - i\,0.150$
A_{κ_2}	$0.385 + i\,0.899$	$0.382 + i\,0.900$
C_κ	$47.853 + i\,33.116$	$46.861 + i\,33.386$
$\Delta\delta_0^{1/2}$	0.026	0.028

$$\Delta\delta_0^{1/2} = \frac{1}{N}\sum_k^N \frac{\left|\delta_0^{1/2,\mathrm{Theo.}}(s_k) - \delta_0^{1/2,\mathrm{Exp.}}(s_k)\right|}{\delta_0^{1/2,\mathrm{Exp.}}(s_k)}$$

Modeling πK scattering with

$$T_0^{1/2}(s) = \frac{\rho(s)}{2}\left[C_\kappa + \sum_{i=1}^{2}\frac{A_{\kappa_i}\left(2m_{\kappa_i}\Gamma_{\kappa_i}\right)}{\rho_{0i}\left(m_{\kappa_i}^2 - s\right) - i m_{\kappa_i}\Gamma_{\kappa_i}\rho_{0i}}\right]$$

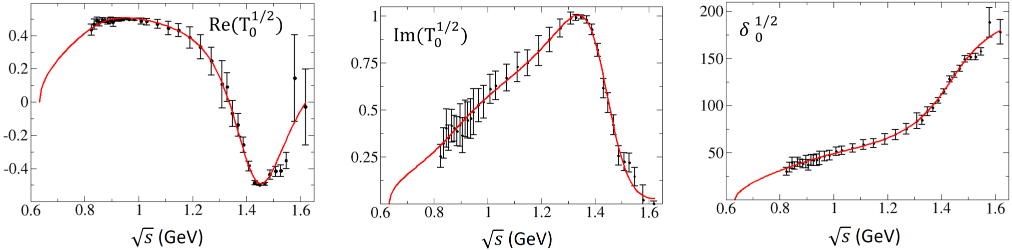

Modeling πK scattering with

$$T_0^{1/2}(s) = \frac{\rho(s)}{2}\left[C_\kappa + \sum_{i=1}^{2} \frac{A_{\kappa_i}\left(2m_{\kappa_i}\Gamma_{\kappa_i}\right)}{\rho_{0i}(m_{\kappa_i}^2 - s) - i m_{\kappa_i}\Gamma_{\kappa_i}\rho(s))}\right]$$

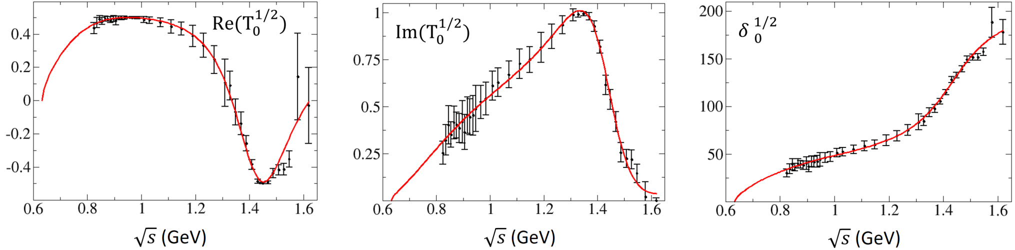

Background-Resonance Interference Approximation

- For the **isotriplets**, we apply two similar models

$$T_0^1(s) = \frac{\rho(s)}{2}\left[C_a + \sum_{i=1}^{2} \frac{A_{a_i}\left(2m_{a_i}\Gamma_{a_i}\right)}{\rho_{0i}(m_{a_i}^2 - s) - im_{a_i}\Gamma_{a_i}\rho_{0i}}\right],$$

$$T_0^1(s) = \frac{\rho(s)}{2}\left[C_a + \sum_{i=1}^{2} \frac{A_{a_i}\left(2m_{a_i}\Gamma_{a_i}\right)}{\rho_{0i}(m_{a_i}^2 - s) - im_{a_i}\Gamma_{a_i}\rho(s))}\right],$$

where $\rho(s) = \frac{q}{8\pi\sqrt{s}} = \frac{\sqrt{[s-(m_\pi+m_\eta)^2][s-(m_\pi-m_\eta)^2]}}{16\pi s}$ and $\{C_a, A_{a_i}\} \in \mathbb{C}$

- Instead of fitting to experimental $\pi\eta$ scattering data, we fit to model-generated data[2]

[2] D. Black, A.H. Fariborz and J. Schechter, Phys. Rev. D 61, 074030 (2000)

- Fitting to model-generated data is similar for both fitting models.

Parameter	Model 1	Model 2
A_{a_1}	$0.864 - i\,0.298$	$0.872 - i\,0.288$
A_{a_2}	$0.726 - i\,0.641$	$0.710 - i\,0.635$
C_a	$-42.7 + i\,17.6$	$-43.0 + i\,19.9$

Modeling $\pi\eta$ scattering with

$$T_0^1(s) = \frac{\rho(s)}{2}\left[C_a + \sum_{i=1}^{2} \frac{A_{a_i}\left(2m_{a_i}\Gamma_{a_i}\right)}{\rho_{0i}(m_{a_i}^2 - s) - i m_{a_i}\Gamma_{a_i}\rho_{0i}}\right],$$

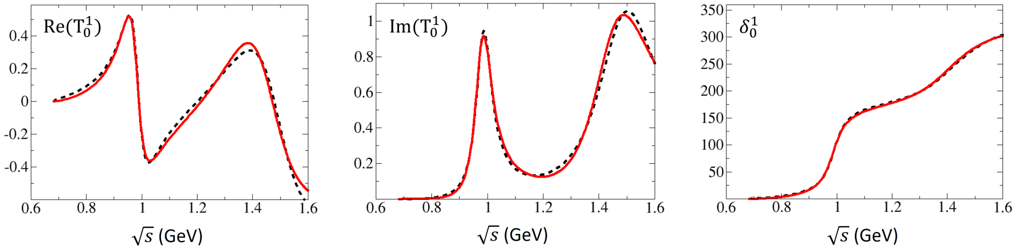

Modeling $\pi\eta$ scattering with

$$T_0^1(s) = \frac{\rho(s)}{2}\left[C_a + \sum_{i=1}^{2} \frac{A_{a_i}\,(2m_{a_i}\Gamma_{a_i})}{\rho_{0i}(m_{a_i}^2 - s) - i m_{a_i}\Gamma_{a_i}\rho(s))}\right],$$

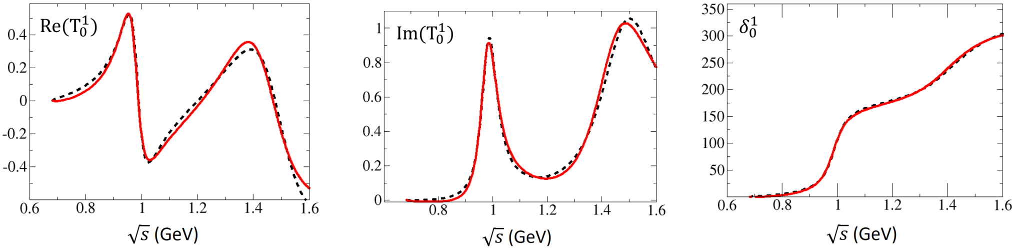

Resonance Models

- QCD Gaussian Sum-rules:

$$\mathcal{G}^{\mathrm{QCD}}\left(\hat{s},\tau,s_0\right) = G^{\mathrm{res}}\left(\hat{s},\tau\right) = \frac{1}{\sqrt{4\pi\tau}} \int_{t_0}^{\infty} dt \exp\left[\frac{-(\hat{s}-t)^2}{4\tau}\right] \varrho^{\mathrm{res}}(t)$$

where $\mathcal{G}^{\mathrm{QCD}}\left(\hat{s},\tau,s_0\right) = G^{\mathrm{QCD}}\left(\hat{s},\tau\right) - \frac{1}{\sqrt{4\pi\tau}} \int_{s_0}^{\infty} dt \exp\left[\frac{-(\hat{s}-t)^2}{4\tau}\right] \frac{1}{\pi}\mathrm{Im}\Pi^{\mathrm{QCD}}(t)$ represents the QCD description.

- We use a resonance + continuum model for the hadronic side of QCDSR where $\varrho^{\mathrm{res}}(t)$ represents fitted input of experimental scattering data.

Model Name	Abbreviation	$\varrho_i^{\mathrm{res}}(t)$
Narrow Resonance	NR	$\delta\left(t-m_i^2\right)$
Propagator Resonance	PROP	$\frac{m_i\Gamma_i}{\left(t-m_i^2\right)^2+m_i^2\Gamma_i^2}$
Distorted Breit-Wigner ($\xi_i=0$)	DBW	$\frac{\rho(t)m_i\Gamma_i}{\left(t-m_i^2\right)^2+m_i^2\Gamma_i^2}$
Generalized Breit-Wigner ($\xi_i=0$)	GBW	$\frac{m_i G_i(t)^2}{\left(t-m_i^2\right)^2+m_i^2 G_i(t)^2}$
Extended Distorted Breit-Wigner	EDBW	$\frac{\rho(t)m_i\Gamma_i}{\left(t-m_i^2\right)^2+m_i^2\Gamma_i^2}+\xi_i\frac{\rho(t)\left(m_i^2-t\right)}{\left(t-m_i^2\right)^2+m_i^2\Gamma_i^2}$
Extended Generalized Breit-Wigner	EGBW	$\frac{m_i G_i(t)^2}{\left(t-m_i^2\right)^2+m_i^2 G_i(t)^2}+\xi_i\frac{G_i(t)\left(m_i^2-t\right)}{\left(t-m_i^2\right)^2+m_i^2 G_i(t)^2}$

Models are arranged in order of increasing sophistication and increasing width effects $(G_i(t)=\rho(t)\Gamma_i/\rho_{0i})$.

Results

- Scale factors $\{\Lambda, \Lambda'\}$ are extracted for each resonance model over an energy scale $0 < \hat{s} < 6\,\mathrm{GeV}^2$. Previously used value of GSR parameter $\tau = 3\,\mathrm{GeV}^4$ used in analysis.
- In order to compare with previous work, each resonance is normalized to the "propagator" model (PROP).
- We define Δ as a measure of universality comparing how the individually determined scale-factors compare within each nonet:

$$\Delta = \left|\frac{\Lambda_\kappa - \Lambda_a}{\Lambda_\kappa + \Lambda_a}\right| + \left|\frac{\Lambda'_\kappa - \Lambda'_a}{\Lambda'_\kappa + \Lambda'_a}\right| .$$

Model	Channel	$s_0^{(1)}$	$s_0^{(2)}$	Λ	Λ'	$\chi^2_\Lambda \times 10^6$	$\chi^2_{\Lambda'} \times 10^6$	Δ
PROP	K_0^*	2.76	1.79	0.1256	0.2798	17.9	19.6	0.0586
	a_0	2.40	2.13	0.1169	0.2928	27.1	6.83	
DBW	K_0^*	2.90	2.11	0.1284	0.2973	14.4	21.0	0.0397
	a_0	2.49	2.20	0.1191	0.2960	27.0	7.33	
GBW	K_0^*	2.97	2.30	0.1297	0.3070	15.6	28.5	0.0539
	a_0	2.53	2.24	0.1201	0.2978	29.1	8.26	

Model	Channel	$s_0^{(1)}$	$s_0^{(2)}$	Λ	Λ'	$\chi^2_\Lambda \times 10^6$	$\chi^2_{\Lambda'} \times 10^6$	Δ
PROP	K_0^*	2.76	1.79	0.1256	0.2798	17.9	19.6	0.0586
	a_0	2.40	2.13	0.1169	0.2928	27.1	6.83	
EDBW	K_0^*	3.20	2.34	0.1339	0.3091	6.10	14.2	0.0182
	a_0	3.08	2.65	0.1318	0.3156	13.3	6.56	
EGBW	K_0^*	3.31	2.49	0.1358	0.3163	5.28	18.3	0.0119
	a_0	3.14	2.69	0.1330	0.3173	13.2	7.04	

GSRs can distinguish between different resonance models.

For $G^{\text{res}}(\hat{s},\tau) = \frac{1}{\sqrt{4\pi\tau}} \int_{t_0}^{\infty} dt \exp\left[\frac{-(\hat{s}-t)^2}{4\tau}\right] \varrho^{\text{res}}(t)$

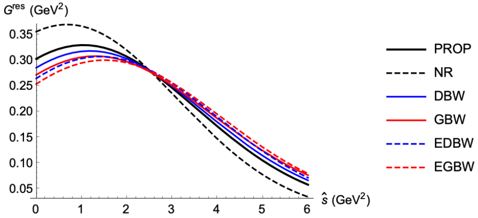

Figure: G^{res} for the $K^*(700)$

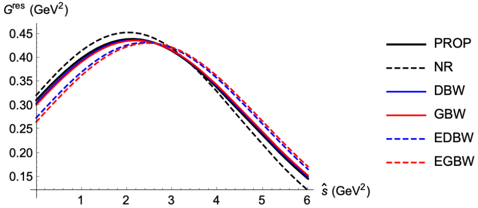

Figure: G^{res} for the $K_0(1430)$

GSRs can distinguish between different resonance models.

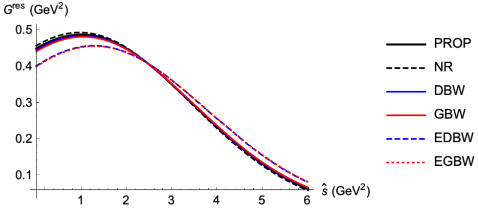

Figure: G^{res} for the $a_0(980)$

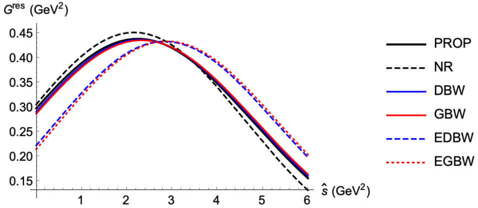

Figure: G^{res} for the $a_0(1450)$

Universality increases as model complexity increases.

Isodoublet:

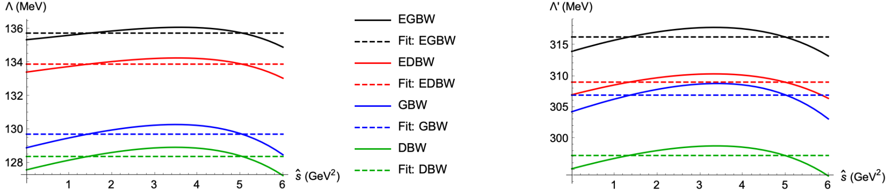

Model	$\chi^2_\Lambda \times 10^6$	$\chi^2_{\Lambda'} \times 10^6$	Δ
EGBW	5.28	18.3	0.0119
EDBW	6.10	14.2	0.0182
GBW	15.6	28.5	0.0539
DBW	14.4	21.0	0.0397

Universality increases as model complexity increases.

Isotriplet:

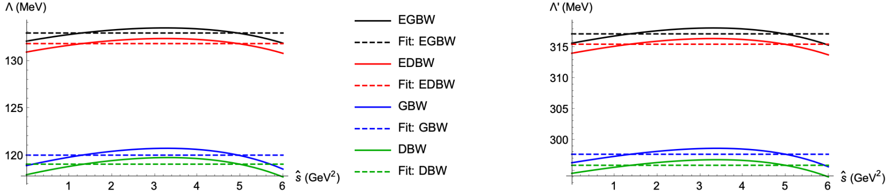

Model	$\chi^2_\Lambda \times 10^6$	$\chi^2_{\Lambda'} \times 10^6$	Δ
EGBW	13.2	7.04	0.0119
EDBW	13.3	6.56	0.0182
GBW	29.1	8.26	0.0539
DBW	27.0	7.33	0.0397

Summary

- We are continuing to develop a methodology relating chiral Lagrangian and QCD sum-rule methodologies.
- Revised Gaussian QCD sum-rule methodology reproduces previous work and opens the possibility of investigating more complex systems.
- New resonance models provide input complex low-energy features and show an improvement in universality.
- Future work includes extension to higher-dimensional isospin sectors, including mixing with glueballs.

Amir H. Fariborz, **JH**, T.G. Steele. Phys. Rev. D 111, 094023. arXiv:2501.12601

Thank You!

$$\mathcal{G}^{\mathrm{QCD}}\left(\hat{s},\tau,s_0\right)=G^{\mathrm{QCD}}\left(\hat{s},\tau\right)-\frac{1}{\sqrt{4\pi\tau}}\int\limits_{s_0}^{\infty}dt\,\exp\left[\frac{-(\hat{s}-t)^2}{4\tau}\right]\,\frac{1}{\pi}\mathrm{Im}\Pi^{\mathrm{QCD}}(t)$$

$$\mathcal{G}^{\mathrm{QCD}}_{(\kappa)11}\left(\hat{s},\tau,s_0\right)=\frac{3}{8\pi^2}\int\limits_0^{s_0} t\,dt\left[\left(1+\frac{17}{3}\frac{\alpha_s}{\pi}\right)-2\frac{\alpha_s}{\pi}\log\left(\frac{t}{\sqrt{\tau}}\right)\right]W\left(t,\hat{s},\tau\right)$$

$$+\frac{\pi n_c\rho_c^2}{m_s^* m_q^*}\int\limits_0^{s_0} tJ_1\left(\rho_c\sqrt{t}\right)Y_1\left(\rho_c\sqrt{t}\right)W\left(t,\hat{s},\tau\right)\,dt$$

$$+\exp\left\{\left(-\frac{\hat{s}^2}{4\tau}\right)\right\}\left[\frac{1}{2\sqrt{\pi\tau}}\left\langle C_4^\kappa\mathcal{O}_4^\kappa\right\rangle-\frac{\hat{s}}{4\tau\sqrt{\pi\tau}}\left\langle C_6^\kappa\mathcal{O}_6^\kappa\right\rangle\right]$$

$$W\left(t,\hat{s},\tau\right)=\frac{1}{\sqrt{4\pi\tau}}\exp\left\{\left(-\frac{\left(t-\hat{s}\right)^2}{4\tau}\right)\right\},\ \left\langle C_4^s\mathcal{O}_4^\kappa\right\rangle=\left\langle m_s\overline{q}q\right\rangle+\frac{1}{2}\left\langle m_s\overline{s}s\right\rangle+\frac{1}{8\pi}\left\langle\alpha_s G^2\right\rangle,$$

$$\left\langle C_6^\kappa\mathcal{O}_6^\kappa\right\rangle=-\frac{1}{2}\left\langle m_s\overline{q}\sigma Gq\right\rangle-\frac{1}{2}\left\langle m_q\overline{s}\sigma Gs\right\rangle-\frac{16\pi}{27}\alpha_s\left(\left\langle\overline{q}q\right\rangle^2+\left\langle\overline{s}s\right\rangle^2\right)-\frac{48}{9}\alpha_s\left\langle\overline{q}q\right\rangle\left\langle\overline{s}s\right\rangle$$

$$\mathcal{G}^{\mathrm{QCD}}_{(\kappa)22}\left(\hat{s},\tau,s_0\right) = \int\limits_0^{s_0} dt\, W\left(t,\hat{s},\tau\right)\, \rho^{\mathrm{QCD}}_{(\kappa)}(t)\,,$$

$$\begin{aligned}
\rho^{\mathrm{QCD}}_{(\kappa)}(t) = {} & \left(\frac{t^4}{11520\pi^6} - \frac{t^3 m_s^2}{572\pi^6}\right) + t^2\left(\frac{\left(7+6\sqrt{2}\right)\left\langle \alpha_s G^2\right\rangle}{2304\pi^5} + \frac{\left\langle m_s \bar{s} s\right\rangle}{72\pi^4}\right) \\
& + t\left(\frac{\left(-7-6\sqrt{2}\right)\left\langle \alpha_s G^2\right\rangle m_s^2}{768\pi^5} + \frac{\left\langle m_s \bar{q}\sigma G q\right\rangle}{128\pi^4}\right) \\
& - \frac{\left\langle \alpha_s G^2\right\rangle\left\langle m_s \bar{q} q\right\rangle}{96\pi^3} + \frac{\left(7+6\sqrt{2}\right)\left\langle \alpha_s G^2\right\rangle\left\langle m_s \bar{s} s\right\rangle}{576\pi^3} - \frac{\left\langle \bar{q}\sigma G q\right\rangle\left\langle \bar{s} s\right\rangle}{48\pi^2} + \frac{\left\langle \bar{q} q\right\rangle\left\langle \bar{s}\sigma G s\right\rangle}{48\pi^2}
\end{aligned}$$

$$\mathcal{G}^{\rm QCD}_{(a)11}\left(\hat{s},\tau,s_0\right) = \frac{3}{8\pi^2}\int_0^{s_0} t\,dt\left[\left(1+\frac{17}{3}\frac{\alpha_s}{\pi}\right)-2\frac{\alpha_s}{\pi}\log\left(\frac{t}{\sqrt{\tau}}\right)\right]W\left(t,\hat{s},\tau\right)$$

$$+\frac{3}{4\pi}\int_0^{s_0} tJ_1\left(\rho_c\sqrt{t}\right)Y_1\left(\rho_c\sqrt{t}\right)W\left(t,\hat{s},\tau\right)\,dt$$

$$+\exp\left\{\left(-\frac{\hat{s}^2}{4\tau}\right)\right\}\left[\frac{1}{2\sqrt{\pi\tau}}\left\langle C_4^a\mathcal{O}_4^a\right\rangle-\frac{\hat{s}}{4\tau\sqrt{\pi\tau}}\left\langle C_6^a\mathcal{O}_6^a\right\rangle\right]$$

$$\left\langle C_4^s\mathcal{O}_4^a\right\rangle = 3\left\langle m_q\overline{q}q\right\rangle+\frac{1}{8\pi}\left\langle\alpha_s G^2\right\rangle\,,\ \left\langle C_6^a\mathcal{O}_6^a\right\rangle = -\frac{172}{27}\alpha_s\left\langle\overline{q}q\right\rangle^2\,.$$

$$\mathcal{G}^{\mathrm{QCD}}_{(a)22}\left(\hat{s},\tau,s_0\right)=\int_0^{s_0} dt\, W\left(t,\hat{s},\tau\right)\,\rho^{\mathrm{QCD}}_{(a)}(t)\,,$$

$$\begin{aligned}\rho^{\mathrm{QCD}}_{(a)}(t) =& \frac{t^4}{11520\pi^6}-\frac{t^3 m_s^2}{288\pi^6}+t^2\left(\frac{\left(7+6\sqrt{2}\right)\left\langle\alpha_s G^2\right\rangle}{2304\pi^5}+\frac{\left\langle m_s\bar{s}s\right\rangle}{36\pi^4}\right)\\ &+t\left(\frac{\left(-7-6\sqrt{2}\right)\left\langle\alpha_s G^2\right\rangle m_s^2}{384\pi^5}-\frac{\left\langle m_s\bar{s}s\right\rangle m_s^2}{6\pi^4}\right)\\ &-\frac{\left\langle\alpha_s G^2\right\rangle\left\langle m_s\bar{q}q\right\rangle}{48\pi^3}+\frac{\left(7+6\sqrt{2}\right)\left\langle\alpha_s G^2\right\rangle\left\langle m_s\bar{s}s\right\rangle}{288\pi^3}+\frac{4\left\langle m_s\bar{q}q\right\rangle^2}{9\pi^2}+\frac{4\left\langle m_s\bar{s}s\right\rangle^2}{9\pi^2}\end{aligned}$$